

Arbeit zur Erlangung des akademischen Grades
Master of Science

Alignment studies for the LHCb SciFi Detector

Nils Breer
geboren in Unna

2022

Lehrstuhl für Experimentelle Physik IV
Fakultät Physik
Technische Universität Dortmund

Erstgutachter: Prof. Dr. Albrecht
Zweitgutachter: Prof. Dr. Weingarten
Abgabedatum: May 4th 2022

Abstract

Kurzfassung

Hier steht das selbe wie im Abstract nur auf deutsch.

Inhaltsverzeichnis

1	Introduction	1
2	Particles and The Large Hadron Collider	2
2.1	The Standard Modell	2
2.2	particle decays and hadrons	4
2.3	The LHC and LHCb	5
2.4	The LHC data cycle	8
3	The Theory of Alignment	9
3.1	Track reconstruction	9
3.2	The Kalman filter method [7]	11
3.3	Alignment using derivatives	13
4	Main part	14
4.1	general info	14
4.2	Nulltests and software tests	15
4.3	chi2 tests and weak modes	23
5	Continuing Work	32
6	Future Work	33
7	Conclusion and Outlook	34
	Literatur	35

1 Introduction

2 Particles and The Large Hadron Collider

2.1 The Standard Modell

The standard model of particle physics describes the known elementary particles and their interactions. It consists of 12 matter particles, the fermions and five interaction particles, which are called vector bosons. The fermions can be grouped in two categories, six quarks and six leptons. The quarks as well as the leptons are divided into three generations. Each matter particle also has an antiparticle, with an opposite charge. The interactions are obtained from the vector bosons mentioned above. The three potent interactions are the electromagnetic(em) interaction, the weak interaction and the strong interaction. Gravitation does not make a significant contribution. The vector boson of the em interaction is the photon which is exchanged between particles. The strength of one of those interactions is described by a coupling constant. In the em interaction this is the fine structure constant[4]. The range of the em-interaction is in principle infinite, but decreases with increasing distance between the interacting particles. The em interaction is described by quantum electrodynamics. The potentials are described by operators, which create and annihilate the photons.

The exchange particles of the weak interaction are on the one hand the W^\pm -bosons and on the other hand the Z-boson. The weak interaction processes are called currents. Changing the charge during the interaction by a W-boson is called charged current. The exchange reaction of a Z boson in, for example, processes such as $e_\nu\mu \rightarrow e_\nu\mu$ is called neutral current. Analogous to the electromagnetic interaction, the potentials are again understood as operators, but here there are no propagators. Propagators are used in *FEYNMAN*-diagrams of QED to represent the interaction particles. A so-called V-A structure is used here instead. Here, V stands for vectorboson and A is the axialvector. This structure is needed to disregard the right-handed particles and left-handed antiparticles, since these lead to the charge-parity violation. Thus one adjusts the Lorentz factors in the following way

$$\gamma_\mu \rightarrow \gamma_\mu(1 - \gamma_5)$$

In the strong interaction, the exchange particles are the eight different gluons. The strong interaction is described by quantum chromodynamics (QCD). According to

this, color is transferred during the interaction. Gluons have no mass and are spin-1 particles. Gluons carry a color and a different anti-color. Gluons can also couple to themselves. Moreover, the coupling constant $\alpha_s \approx 0.1$. The interaction with quarks is described with a potential.

$$V_{q\bar{q}} = -\frac{4\alpha_s}{3r} + \sigma \cdot r \quad (2.1)$$

mit

$$\sigma = 1 \frac{\text{GeV}}{\text{fm}} \quad (2.2)$$

Quarks thus tend to attract each other very strongly. If now quark and antiquark are moved away from each other, a lot of energy has to be expended. This energy can become so large that new particles can be created.

The standard model houses 12 spin- $\frac{1}{2}$ fermions. Six are called leptons and they are sorted into three families, also called flavor (e, μ and τ). Each of those families has a charged lepton¹ and a left-handed neutrino. A particle is called left-handed if its spin direction is opposite to the direction of flight. Right-handed particles have a spin direction pointing with the direction of flight. Therefore, a left-handed isospin doublet and a right-handed singlet is constructed. The leptons can couple via the weak-interaction and if they are charged, also via the em-interaction. Neutrinos can only couple via the weak interaction.

The quarks are spin- $\frac{1}{2}$ -fermions and carry an electric charge as well. In each of the three generations there is one isospin doublet. The quarks are ordered by ascending mass. In the first generation are the two lightest quarks, up- and down quark, in the second generation the charm- and strange quark and in the third generation the top- and bottom quark doublet. Quarks carry a color charge, red, green or blue, which is an artificially introduced degree of freedom to guarantee the distinguishability. Quarks couple via the strong interaction which is described by the quantum chromodynamic (QCD). The Eichgroup of the QCD is $SU(N=3)$ where N is the number of introduced colors. The number of generators is therefore $N^2 - 1 = 8$. The generators are called gluons and they carry "color" and "anticolor".

¹can have both händigkeiten

The common eight gluon-wavefunctions are

$$\begin{aligned}
 \psi_1 &= |r\bar{g}\rangle & \psi_2 &= |r\bar{b}\rangle \\
 \psi_3 &= |g\bar{r}\rangle & \psi_4 &= |g\bar{b}\rangle \\
 \psi_5 &= |b\bar{r}\rangle & \psi_6 &= |b\bar{g}\rangle \\
 \psi_7 &= \frac{1}{\sqrt{2}}(|r\bar{r}\rangle - |g\bar{g}\rangle) & \psi_8 &= \frac{1}{\sqrt{6}}(|r\bar{r}\rangle + |g\bar{g}\rangle - 2|b\bar{b}\rangle)
 \end{aligned}$$

The second wavefunction describes a gluon interaction with a blue quark and changing the color to red.

Due to the Confinement, quarks cannot exist alone. Instead they form bonding states, so called hadrons. On the one hand there are the mesons, which consist of a quark and an antiquark.

$$|M\rangle = |q\bar{q}'\rangle \quad (2.3)$$

These may be from the same family (i.e. [u,d], [c,s], [t,b]), or from different families. Mesons have a baryon number of 0. Accordingly, quarks carry the baryon number $\frac{1}{3}$. The quarks constructing a meson therefore carries color and the corresponding anticolor. The second type are baryons. The content consists of either three quarks or three antiquarks. However, it cannot be that one quark and two antiquarks and vice versa occur, because baryons must have the baryon number $B = 1$. Because baryons are stable final states as well as the mesons, the sum of their quark colors must be white. Therefore, every (anti)color must occur once in a baryon.

$$|B\rangle = |qq'q''\rangle \quad (2.4)$$

$$|B\rangle = |\bar{q}\bar{q}'\bar{q}''\rangle \quad (2.5)$$

2.2 particle decays and hadrons

For you, this is because the bending and momentum of particles (and the location where they decay) is important to the way we can align things. Which sorts of particles can produce long tracks? etc.

2.3 The LHC and LHCb

2.3.1 The LHC

The Large Hadron Collider (LHC)[2] is the most powerful particle-accelerator on planet earth. With a circumference of 26,7km it is also the longest ring accelerator and it lies between 45m and 170m below the surface near Geneva in Switzerland. The tunnel was constructed for the LEP experiment between 1984 and 1989 and is operated by the European Organization for Nuclear Research (CERN). The LHC can produce centre of mass energies of $\sqrt{s} = 13 \text{ TeV}$ in proton-proton collisions during Run 2. After the upgrade the LHC will collide particles with the centre of mass energy $\sqrt{s} = 13 \text{ TeV}$. An image of the accelerators and the experiments is shown in fig. 2.1[1].

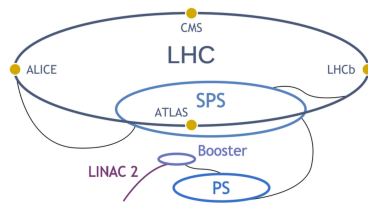


Abbildung 2.1: an overview of the LHC facilities.

By ionizing hydrogen gas, protons are created and accelerated to 50 MeV by the linear accelerator (LINAC 2). Afterwards the beam is injected into the Proton Synchrotron and the Super Proton Synchrotron to a maximum of 450 GeV before the beam is brought into the LHC. The beam contains several bunches with around $1,15 \cdot 10^{11}$ and a bunch spacing of 25 ns, which is a collision rate of 40 MHz. The LHC houses four major experiments. ATLAS and CMS are classified as general purpose detectors with a detection range of close to 4π . The interaction in these detectors is located in the very center so that tracks going in every direction can possibly be found. Searches for the Higgs Boson is just one of many physics aspects these detectors are built for. The other two Experiments located at the LHC are ALICE and LHCb. The ALICE experiment mainly studies the quark gluon plasma during the runs with lead ion collisions instead of protons. In this thesis the Scintillating

Fibre Tracker (SciFi Tracker) located at the LHCb will be focused at and discussed on the following chapters.

2.3.2 The LHCb

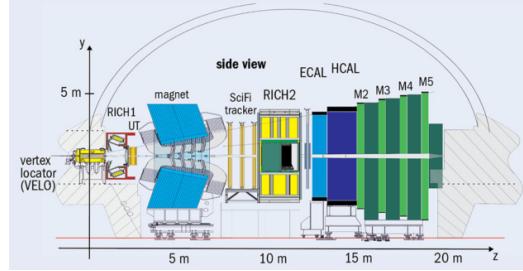


Abbildung 2.2: a sideview of the LHCb experiment.

The LHCb experiment[6] is a forward spectrometer covering $2 < \eta < 5$ in the pseudorapidity range. This experiments main physics goal is beauty quark physics and for high energies, b - and \bar{b} -hadrons are heavily produced in a tight forward direction². A sideview of the LHCb is shown in figure 2.2. The LHCb consists of several smaller detector components namely the Vertex Locator (VELO) right on the intercation point, two Ring Imaging Cherenkov counter (RICH 1 and RICH 2), in front of the spectrometers lies the Trigger Tracker and behind them the SciFi Tracker which is the important part of this thesis. Further back a Scinitllator Pad Detector (SPD) and a Preshower (PS) are mounted followed by the electromagnetic calorimeter (ECAL) and the hadronic calorimeter (HCAL). In the very back, several muon chambers are mounted for every track that is yet to be determined.

In this section, a general overview about the requirements for the SciFi Tracker as well as the layout will be discribed based on the presentation in the *technical design report*[3] of the upgrade.

The upstream and downstream trackers provide a good precision estimate of the momentum of charged particles so that mass resolution of decayed particles can be precisely measured. For particle identification the reconstructed trajectories of charegd particles are used as input for the RICH detectors. The limiting factor for the momentum resolution is multiple scattering for tracks with a momentum lower than 80 GeV/ . For tracks with a higher momentum the detector resolution is the limiting factor.

²They are also produced in a tight backward direction but the experiment is only build for the forward cone.

The SciFi Tracker replaced the inner Tracker (IT) and the outer Tracker (OT) and is located in the same place as the downstream trackers that were previously installed.

The instantaneous luminosity after the upgrade is expected to be $1\text{ 1}/(\text{cm}^2\text{ s})$ bis $2 \cdot 10^{33}\text{ 1}/(\text{cm}^2\text{ s})$. The bunch spacing will be 25 ns and the number of proton-proton interactions per bunch crossing will be $\nu = 3.8$ during the ramp-up phase of the LHC and $\nu = 7.6$ "during the active phase." (how can i write this differently?)

2.3.3 Layout of the SciFi Tracker

The SciFi Tracker consists of three (T-)stations T1, T2 and T3 with each having four layers ($X1, U, V, X2$). The orientation of these planes with respect to the vertical axis are $(0^\circ, 5^\circ, -5^\circ, 0^\circ)$. The tilted layers are called stereo layers and serve the purpose of 3D hit localization. The layers are 20 mm apart from each other in z -direction within each station. Each layer has four quarters with each quarter having five³ modules. Each module is constructed from four fibre mats. A right-handed coordinate system is used with positive z pointing away from the interaction point following the beam direction. positive y points upwards, towards the surface and positive x and negative x are defined as A-Side and C-Side[3].

To ensure an optimal alignment, a well known geometry is key. Therefore, the fibres must aligned within $50\text{ }\mu\text{m}$ bis $100\text{ }\mu\text{m}$ in x -direction and must not be more than $300\text{ }\mu\text{m}$ bent in z -direction.

2.3.4 Scintillating Fibres

The scintillating fibre material is a polymer with an organic flourescent dye added to the polystyrene structure to enhance the yield during the scintillation process. In order to produce and register a photon signal, the ionisation energy is deposited in the fibre core firstly. The amount of energy need for the polymer to reach an excited state is just a few electronvolts. The added dye has the particular structure to match the excitation energy. The energy is transferred via the Förster Transfer. The dye generates excited energy states when particles hit the fibre and deposit their energy. When the states relax, a photon is emitted which then excites other parts of the dye to eventually transfer the energy to the silicon photomultipliers (SiPMs) which are mounted on the outer(?) end of the mats. The other end of the fibre mats is a full reflective mirror to send the photons towards the SiPMs.

³six for the last (T-)station.

2.4 The LHC data cycle

(not sure if that's a good name, but like, an explanation of how electrical information is turned into hits and then tracks, and also when alignment runs in the system of data taking)

3 The Theory of Alignment

here comes the theory part for general alignment

3.1 Track reconstruction

In order to function optimally, the LHCb detector stands before a difficult duty. The track reconstruction algorithm needs to find the correct hits from each subdetector to build the track. This can be problematic just because of the amount of tracks per events (roughly 100). It is crucial to find all particle tracks and also their track parameters which come from the track fit.

A good track fit is needed in order to find to best estimates for the track parameters and covariances. The estimates are used in the event reconstruction to find the correct tracks for each particle and the decay products. The info provided is used in the RICH rings, ECAL and HCAL and muon detectors. With these information, particle and track parameters such as the invariant mass can be measured and vertex origins can be found. There are several track models that can be used. In general, a track is build from numnerous segments which are either straight or curved because of an active magnetic field. Depending on the environment of the track either model is good. The track segments are called track states and are defined by a position in x and y at a given distance z where the hit was located, then a tanget direction $t_{x,y}$ at the hit position and a momentum parameter acquired from the track curve inside the magnetic field.[7]

$$\vec{r} = \begin{pmatrix} x \\ y \\ t_x \\ t_y \\ \frac{q}{p} \end{pmatrix} \quad t_x = \frac{\partial x}{\partial z} \quad t_y = \frac{\partial y}{\partial z} \quad (3.1)$$

The uncertainty of the five-component state vector is a 5×5 covariance matrix C . A track state can be anywhere on the trajectory but is easier to choose it at

3 The Theory of Alignment

real detection points. Combining the track state with a real measurement point is called *node*. The propagation from node $k-1$ to node k is described by a propagation function

$$\vec{r}_k = f_k(\vec{r}_{k-1}) + \vec{w}_k \quad (3.2)$$

.

This means node k is acquired by propagating node $k-1$ through the propagation function f_k and shifting it by the *process noise* \vec{w}_k . Process noise can be caused by any scattering phenomenon that may have happened.

Depending on the type of propagation, linear or curved, a different propagation function is used. for a linear extrapolation, f_k results in

$$f_k(\vec{r}_{k-1}) = F_k \vec{r}_{k-1} \quad (3.3)$$

with the transport matrix F_k

$$F_k = \begin{pmatrix} 1 & 0 & \Delta z & 0 & 0 \\ 0 & 1 & 0 & \Delta z & 0 \\ 0 & 0 & 1 & 0 & 0 \\ 0 & 0 & 0 & 1 & 0 \\ 0 & 0 & 0 & 0 & 1 \end{pmatrix} \quad (3.4)$$

and Δz being the difference in z between the nodes

$$\Delta z = z_k - z_{k-1} \quad (3.5)$$

Trajectory information for each node is provided by the real measurement where the relation between measurement m_k and track state at a given node k is defined as

$$m_k = h_k(\vec{r}_k) + \epsilon_k \quad (3.6)$$

with the projection function h_k and *measurement noise* ϵ_k . So if the detector only measures the y coordinate of state, the projection function will be

$$h_k(\vec{r}_k) = H_k \vec{r}_k \quad (3.7)$$

with

$$H_k = \begin{pmatrix} 0 & 1 & 0 & 0 & 0 \end{pmatrix} \quad (3.8)$$

When measuring more parameters the measurement matrix H_k and projection matrix have dimension $n \times 5$ with n being the numbers of parameters measured.

With this track model, both noises from the measurement and the process are random and unknown and have an expectation value of zero. They are defined as $W_k \equiv \text{cov}(w_k)$ and $V_k \equiv \text{cov}(\epsilon_k)$.

3.2 The Kalman filter method [7]

In general a track is an ensemble of measurements and track states and the Kalman filter method is used to fit tracks. The idea of the Kalman filter is, to have a starting node and add measurements one by one. In between the addition of measurements, the local track state is updated with the new information. The Kalman filter method is a χ^2 minimising problem for the measurement of the track. Because of the iterative nature of the method, it is fast und also used in other fields than physics, for example GPS and meteorology. The three steps of the Kalman filter will be briefly outlined and later discribed in further detail.

The first step is the Prediction: The next track state of the trajectory is predicted based on the track state at the previous node. The second step is the Filter procedure: By using filter equations, the prediction is updated with measurement information in this node. The prediction and filter are repeated for each measurement. With more measurements added, the estimate for the best trajectory is the track state after each filter step. The final step is called Smoother: When the trajectory is complete, smoother equations are applied from the last node to the previous node. Therefore the information from all measurements is used in both forward- and backpropagation which results in a "smoother" track.

3.2.1 1. Step: Prediction

For a given state vector at node $p-1$, the prediction for the p^{th} state vector and its covariance matrix results from the propagation relations

$$\vec{r}_p^{p-1} = f_p(\vec{r}_{p-1}) \quad (3.9)$$

$$\text{Cov}_p^{p-1} = F_p C_{p-1} F_p^T + Q_k \quad (3.10)$$

The superscript of the statevector shows the number of measurements used in the estimate and can be abbreviated with $\vec{r}_p^p \equiv \vec{r}_p$. For a maximum number of n measurements \vec{r}_p^n is the smoothed state where every measurement is used. Q_p is the process noise in matrix form and it is part of the predicted covariance matrix C_p^{p-1} . Because the first state cannot take measurements from the previous state, an initial prediction is taken from the track finding algorithm instead. The predicted residual between the measurement, m_p and the state vector results in

$$\text{res}_p^{p-1} = m_p - h_p (\vec{r}_p^{p-1}) \quad (3.11)$$

and the corresponding covariance matrix is defined as

$$\text{Cov}_{\text{res},p}^{p-1} = V_p + H_p C_p^{p-1} H_p^T \quad (3.12)$$

.

Here, V_p is the measurement variance. With these metrics the minimal χ^2 for the optimal track states can be calculated via

$$(\chi^2)_p^{p-1} = \text{res}_p^{p-1} (\text{Cov}_{\text{res},p}^{p-1})^{-1} \text{res}_p^{p-1} \quad (3.13)$$

3.2.2 2. Step: Filter

During the filter step, the track state is updated with the measurement information. Iteratively, each measurement is added and the filtered state \vec{r}_p and the corresponding covariance matrix is calculated via

$$\vec{r}_p = \vec{r}_p^{p-1} + G_p \text{res}_p + p^{p-1} \quad (3.14)$$

$$\text{Cov}_p = (\mathbb{1} - G_p H_p) \text{Cov}_p^{p-1} \quad (3.15)$$

, where G_p is the gain matrix of dimension 5×1 and is defined as

$$G_p = C_p^{p-1} H_p^T (\text{Cov}_{\text{res},p}^{p-1})^{-1} \quad (3.16)$$

Afterwards the residuals and its covariance matrix are calculated and the filtered total χ^2 is defined as

$$(\chi_{\text{filter}}^2)_p = \text{res}_p \text{Cov}_{\text{res},p}^{-1} \text{res}_p \quad (3.17)$$

.

The prediction and filter procedure is continued for all measurements until the track is fully reconstructed. Because the last node at $p = n$ has the most information in it, a backward update is performed to infuse the previous nodes with the same information as in last node. This is called *smoother*-step.

3.2.3 3. Step: Smoother

The smoother function returns the best possible estimate for track states at the previous nodes. The method used is called *Rauch-Tung-Striebel*-smoother. The idea is to use backward information and construct a smoothed state vector and covariance matrix

$$\tilde{r}_p^n = \vec{r}_p + S_p (\vec{r}_{p+1}^n - \vec{r}_{p+1}^p) \quad (3.18)$$

$$\tilde{C}_p^n = C_p \quad (3.19)$$

and the Smoother-matrix S_p of dimension 5×5

$$S_p = C_p F_{p+1}^T (C_{p+1}^p)^{-1} \quad (3.20)$$

In order to calculate the smoothed χ^2 the residual and corresponding covariance matrix are

$$\text{res}_p = m_p - h_p \vec{h}_p^n \quad (3.21)$$

$$\text{Cov}_{\text{res},p}^n = V_p - H_p C_p^n H_p^T \quad (3.22)$$

An in depth explanation is given in [5].

The χ^2 is calculated analogously to the one during the filter step with the difference being the new residuals and covariances.

3.3 Alignment using derivatives

4 Main part

4.1 general info

Alignment using tracks and vertices regarding stations layers and modules. testing constraints for different degrees of freedom with the goal to find the "perfect" configuration of constraints and alignable degrees of freedom. Used the pre-installed alignment conditions with the survey constraints being "FT : 0 0 0 0 0 0 : 1 1 1 0.0003 0.0003 0.0003"

"FT/T. : 0 0 0 0 0 0 : 1 1 1 0.0003 0.0003 0.0003"

"FT/T./Layer(X1|U|V|X2) : 0 0 0 0 0 0 : 0.2 0.2 0.2 0.0001 0.0001 0.0001"

"FT/.*Module. : 0 0 0 0 0 0 : 0.1 0.1 0.1 0.001 0.001 0.001"

"FT/.*Mat. : 0 0 0 0 0 0 : 0.05 0.05 0.05 0.1 0.1 0.1".

The string is the name of the element, the first set of six numbers are hardcoded parameters for each of the 3 translation degrees of freedom and 3 rotational degrees of freedom (Tx, Ty, Tz, Rx, Ry, Rz) and the second set of six parameters are the corresponding uncertainties. The scale for the translations are mm and the scale for the rotations being rad. A survey uncertainty of 0,0001 stands for 0,1 mrad.

The alignments have been performed with gaudisplitter.

During the Alignment, lagrange constraints can be utilized to minimize the χ^2 under the condition

$$f(\alpha) = 0 \quad (4.1)$$

and adding the lagrange parameter Λ to get

$$\Delta\chi^2 = \Lambda f(\alpha) \quad (4.2)$$

.

Lagrange constraints are added to fix losely constrained degrees of freedom and can be used for any linear combination of movements.

include table from <https://twiki.cern.ch/twiki/bin/view/LHCb/TAlignmentManual>.

4.2 Nulltests and software tests

As a starting point, Alignment v17r1 was used for 5000 events with the magnet in upward position and *GoodLongTracks* (was sind goodlong tracks? definition von cuts etc.)

Results: (sort under the right plots)

- Alignment with Rz (and Rx) takes lots of iterations to converge
- increasing nEvents does not improve it →weak mode?

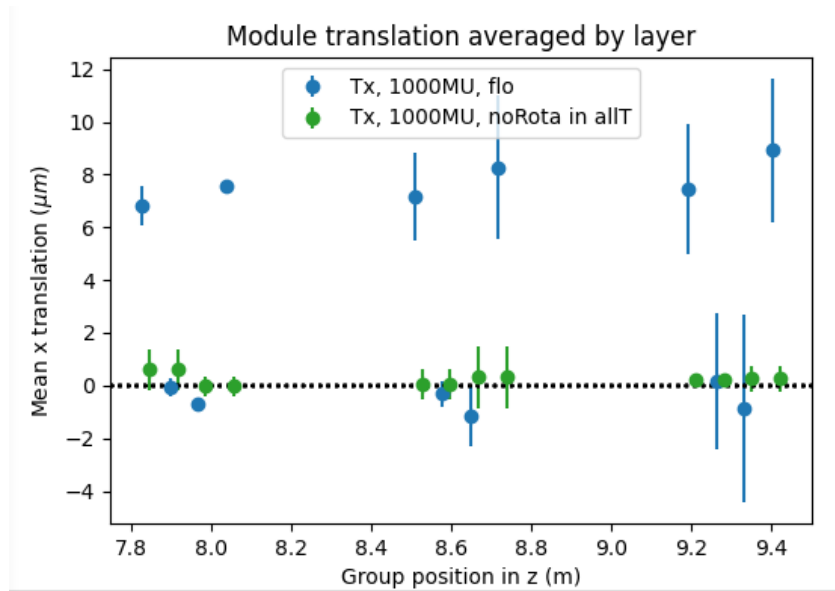


Abbildung 4.1: comparison of different configurations without rotational constraints in every station, magnet up and 1000 events. plotted is translation in x versus global z.

maybe show this plot 4.3

the figure in 4.4 shows that very strict Tx constraints make Tx look better but when comparing to Tz as we can see in figure 4.5 a clear layer separation is visible. because of the many constraints that are applied to T3, a compensation is happening in the other two stations.

Looking at figure 4.6, the last two layers in station 3 are separation from the first two. Especially the last station should be fixed around zero with the constraints added.

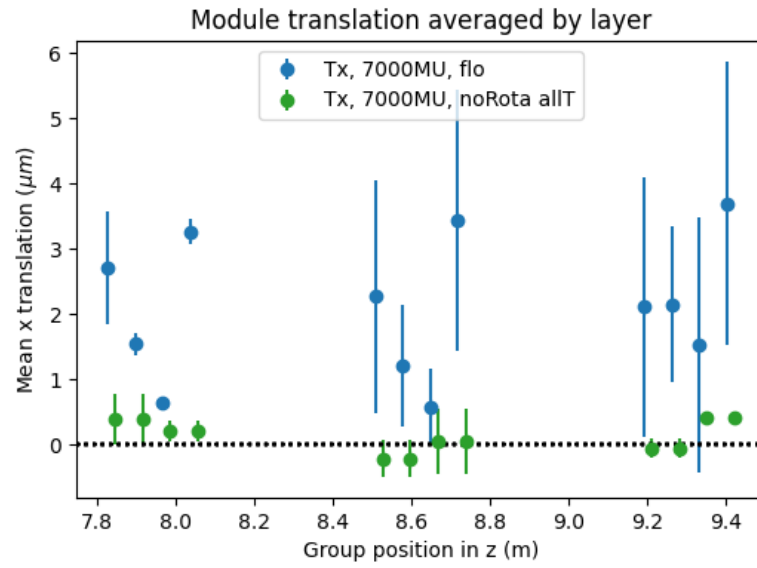


Abbildung 4.2: comparison of different configurations without rotational constraints in all stations, magnet up and 7000 events. plotted is x translation versus global z.

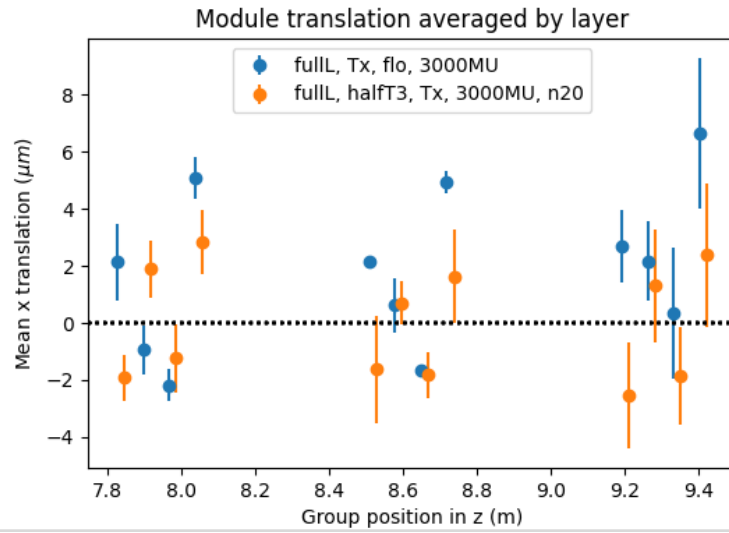


Abbildung 4.3: analysed 20 iterations for x translation behavior (look up exact constraints and dofs)

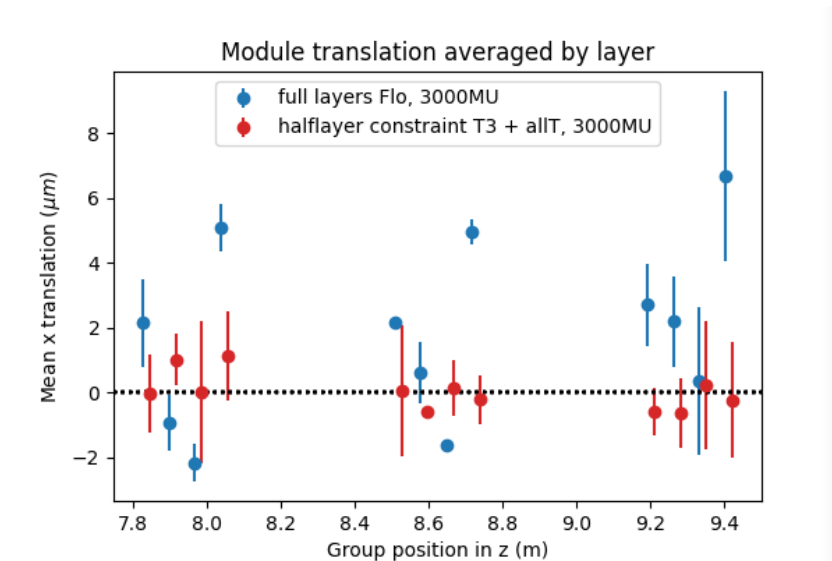


Abbildung 4.4: halflayer constraints and full layer constraint, very strict (look up exact constraints and dofs)

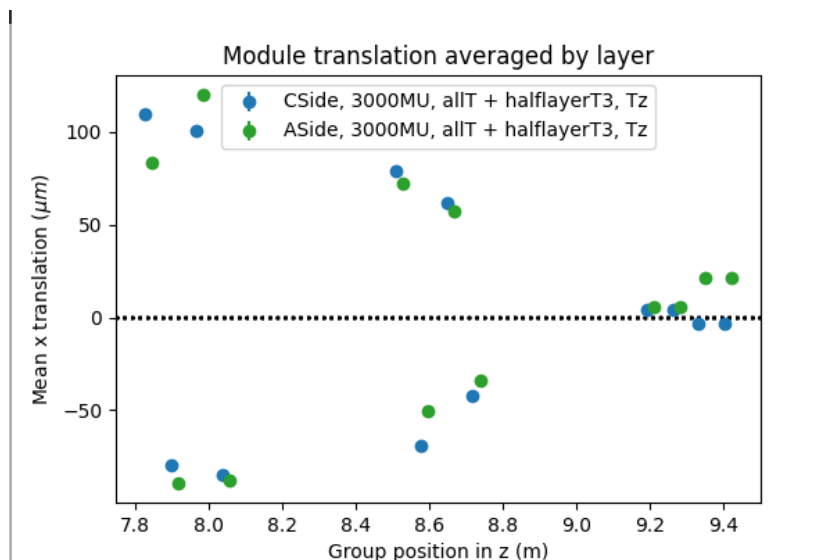


Abbildung 4.5: compare C-Side to A-Side for Translation in z direction. (look up exact constraints and dofs)

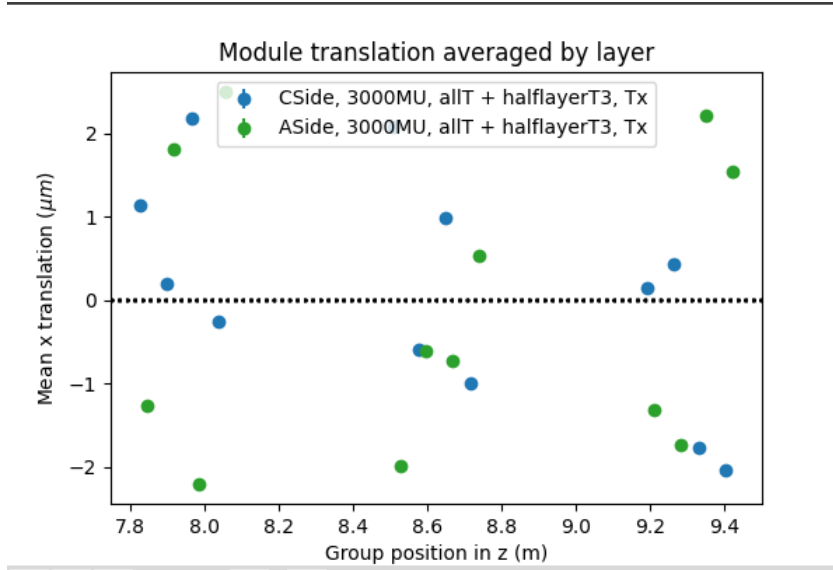


Abbildung 4.6: compare C-Side to A-Side for Translation in x direction. (look up exact constraints and dofs)

The sum of all translations should be zero with each individual layer movement being small.

test 3:

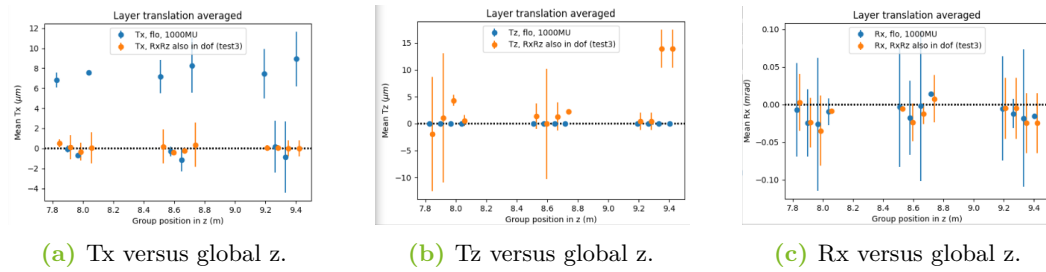


Abbildung 4.7: Testing a configuration versus florians changes.

update: constraining backlayer and also aligning it (append dofs by : Rx Rz) Results:

- improves null tests for Rz but not the only reason why its shifted (cluster bias! expand later)
- shearing and scaling constraints do NOT improve this

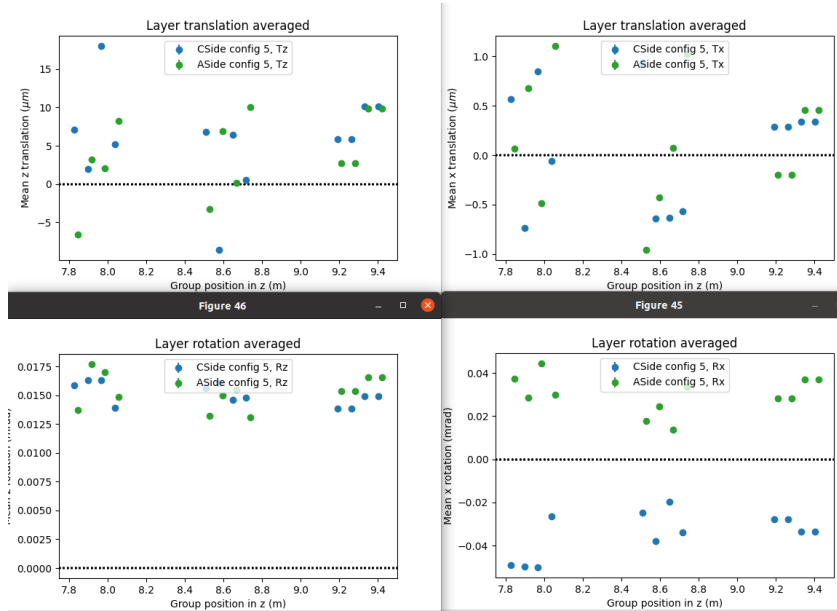


Abbildung 4.8: old config 5, plotted C and ASide.

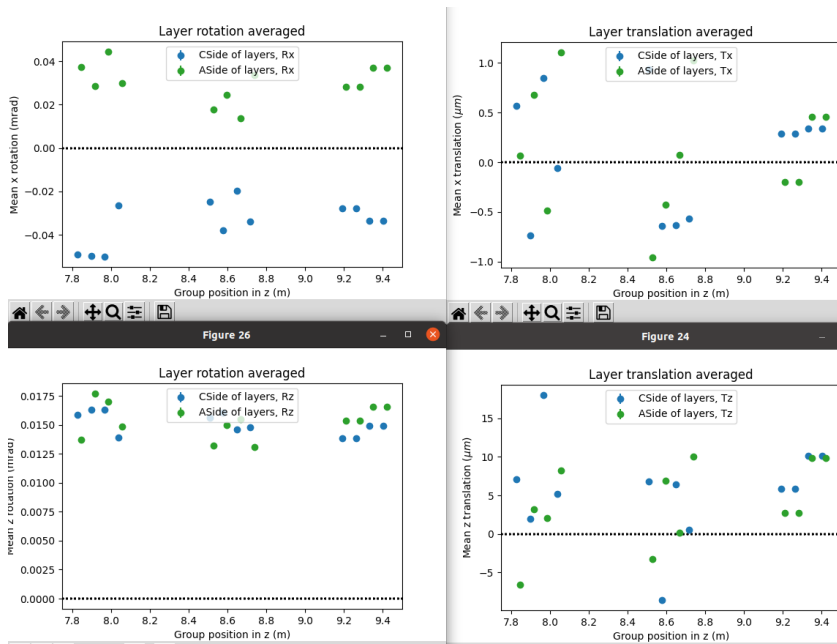


Abbildung 4.9: new config 5, plotted C and ASide.

4 Main part

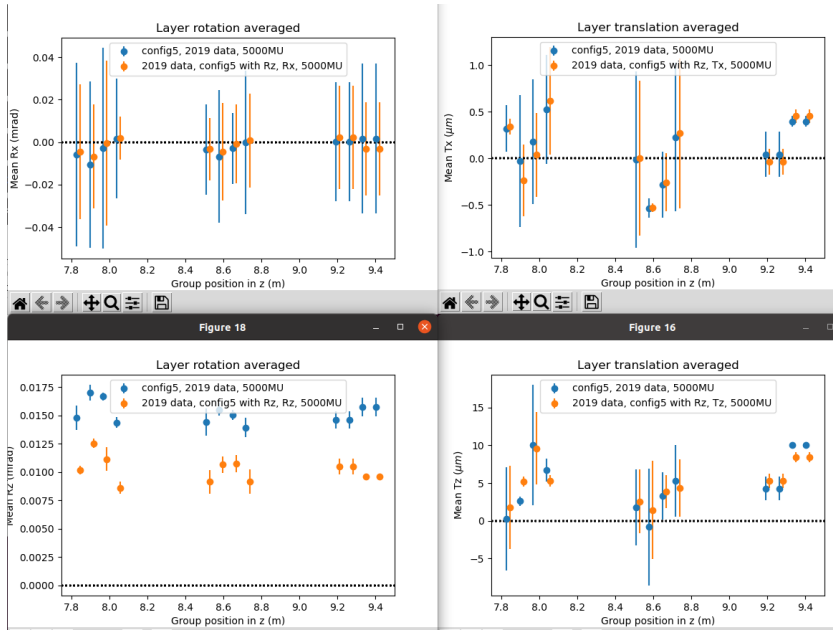


Abbildung 4.10: config5 versus config 5 with Rz constraint for rotational improvement.

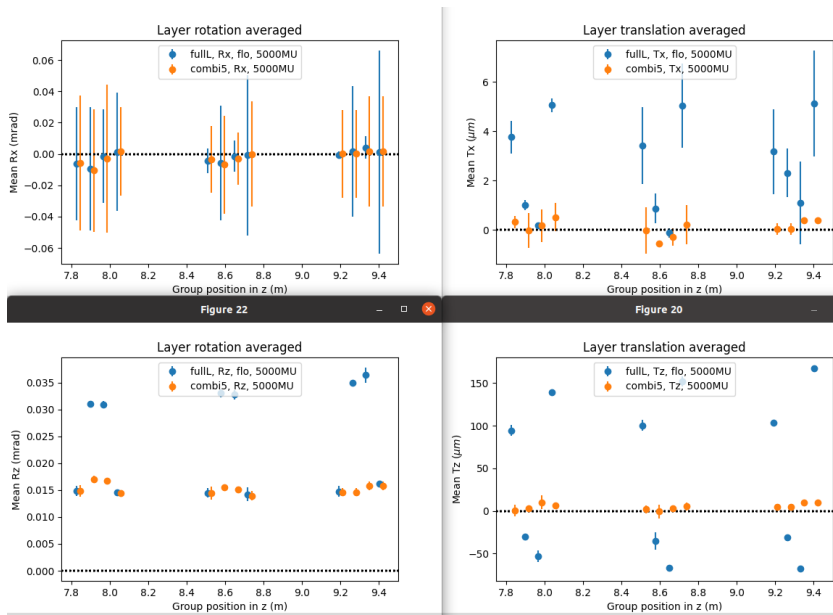


Abbildung 4.11: flo with full layer constraint versus config 5

```
# configure the alignable degrees of freedom
from Alignment.Alignables import *
elements = Alignables()
dofs = "TxTzRxRz"

elements.FTStations(dofs)
elements.FTFrameLayers(dofs)

from Configurables import TAlignment
TAlignment().ElementsToAlign = list(elements)
TAlignment().VertexLocation = "Rec/Vertex/Primary"

from Alignment.TrackSelections import *
TAlignment().TrackSelections = [GoodLongTracks()]
TAlignment().WriteCondSubDetList = [ 'FT' ]

from Configurables import SurveyConstraints
surveyconstraints = SurveyConstraints()
surveyconstraints.FT()

# add survey constraints here:
#TAlignment().SurveyConstraints = surveyconstraints
#surveyconstraints.append("/.*?/FT/.*/M. : 0.0 0.0 0.0 : 0.1 0.1 0.1 0.0001 0.0001 0.0001")
constraints = []
TAlignment().Constraints = constraints

# list of constraints
# constraints = ["Layers : FT/T.*Layer(X1|U|V|X2).Side : Tx Ty Tz Rx Ry Rz"]
# constraints.append("Stations : FT/T.*Layer(X1|U|V|X2).Side : Tx Tz")
# constraints.append("Stations : FT/T. : Tx Tz Rx Rz")
constraints.append("station3 : FT/T3 : Tx Tz Rx Rz")
constraints.append("backlayer_T3 : FT/T3/Layer(V|X2) : Tx Tz")
#constraints.append("station2 : FT/T2 : Tx Tz")
#constraints.append("station1 : FT/T1 : Tx Tz")

# T3
Quarter[0][2] : Tx Tz Rx Rz"
constraints.append("FT/T3VX2CSide : /dd/Structure/LHcb/AfterMagnetRegion/T/FT/T3/Layer(V|X2)/QuarterS
```

Abbildung 4.12: constraints for combi 5 used.

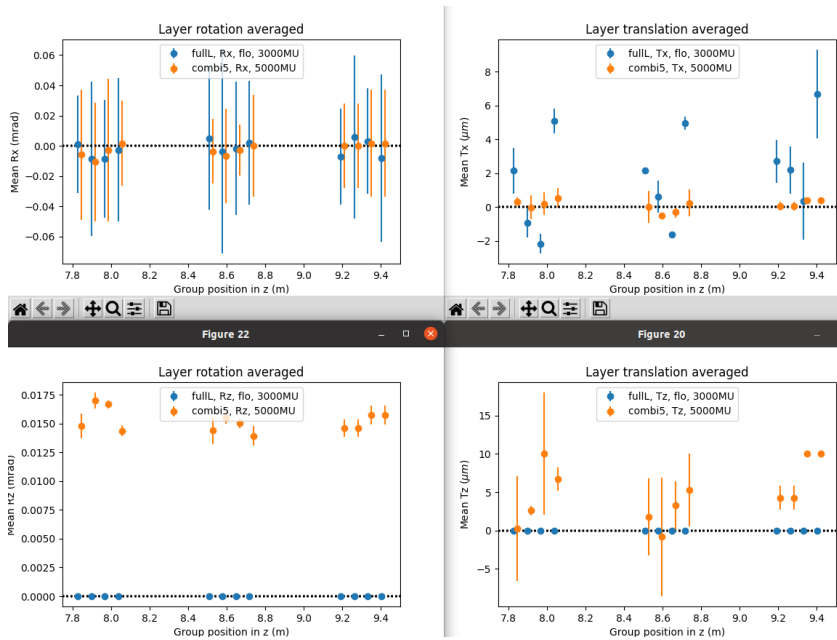


Abbildung 4.13: original new config 5, should be the first good plot to show!!

4 Main part

Results of 100mu translation misalignment:

100mu translation misalignment matches expected survey uncertainty. BUT layers shifted from 0 ! TODO: FTTrackmonitor to study later splitting in track output

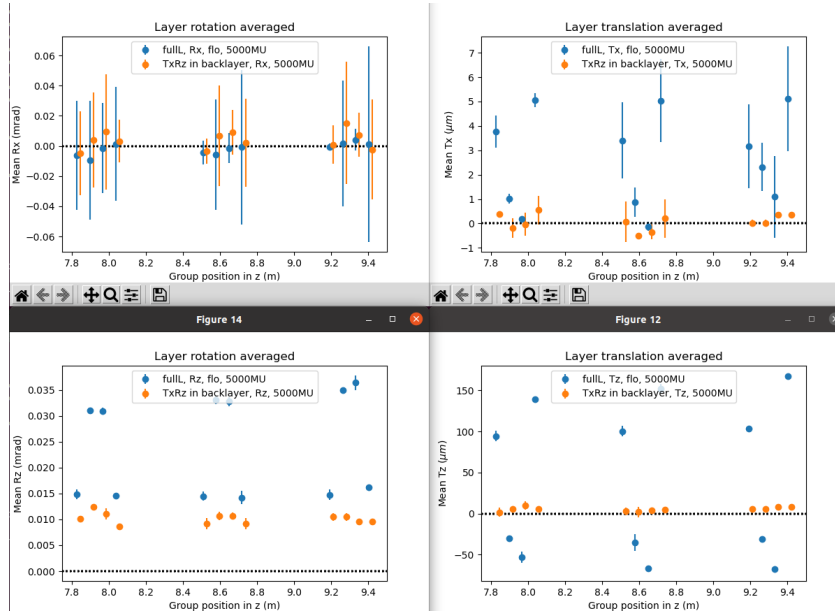


Abbildung 4.14: dofs Tx Rz and backlayer constraints.

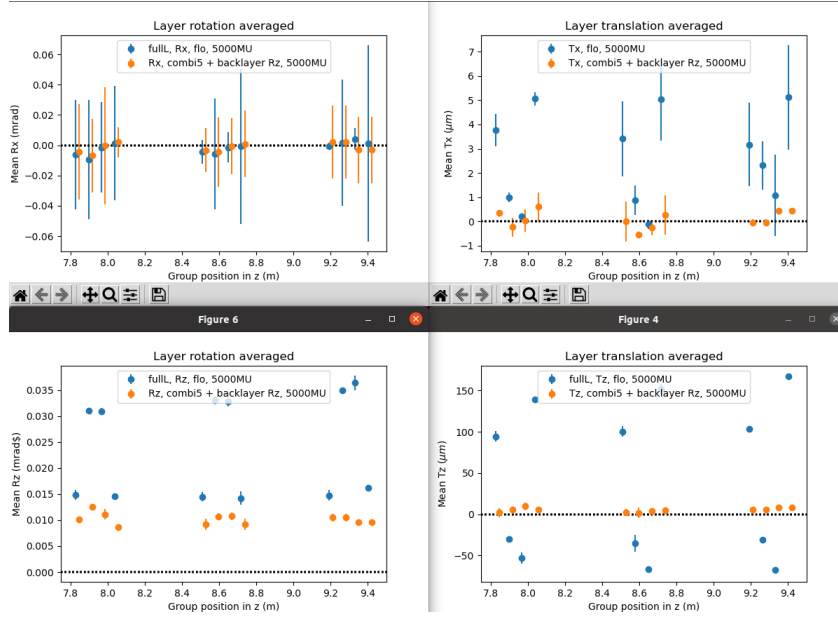


Abbildung 4.15: combi 5 with Rz backlayer constraint.

4.3 chi2 tests and weak modes

In this section, χ^2 are performed in order to study the "goodness" of the alignment since the better the χ^2 after the alignment the better. The second aspect i want to cover is the impact of potential weak modes also known as "correlated alignment parameters". There are several weak modes that could occur namely *global translation*, *shearing* and *curvature bias*. weak modes are unaffected by the χ^2 since the residuals do not change. The effect weak modes have on the alignment are biases regarding track parameters and late convergences. There are different solutions that can be utilized to reduce the effect from weakmodes such as

- *using other configurations like magnet off for mass plots for off-axis events*
- *utilizing other survey datasets*
- *using kinematic and vertex constraints*

january 17th plots are for luminosity comparisons. nu for ramp up luminosity versus lumi during data taking.

for figure 4.23 redo the plot with correct labels!!

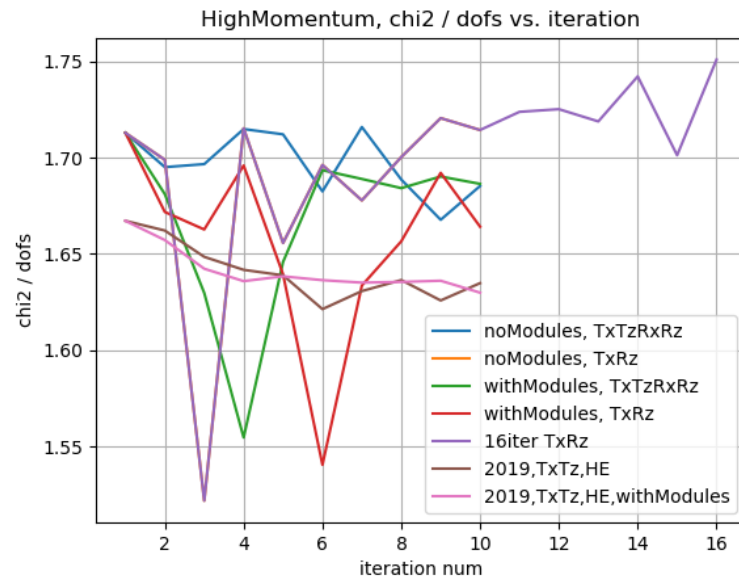


Abbildung 4.16: chi2 vs iteration count.

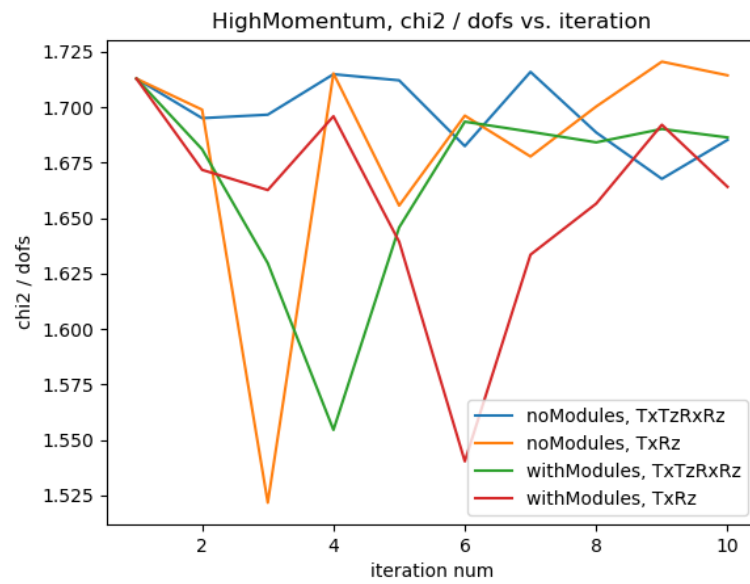


Abbildung 4.17: chi2 versus iteration count.

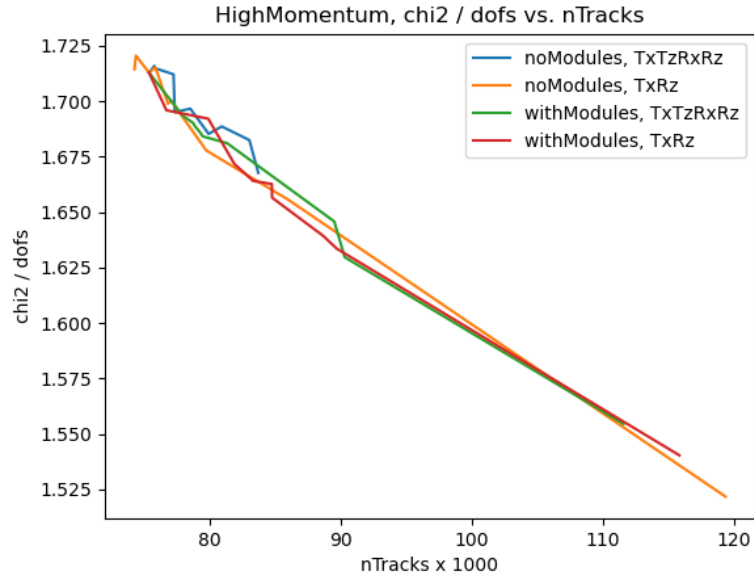


Abbildung 4.18: χ^2 versus number of tracks.

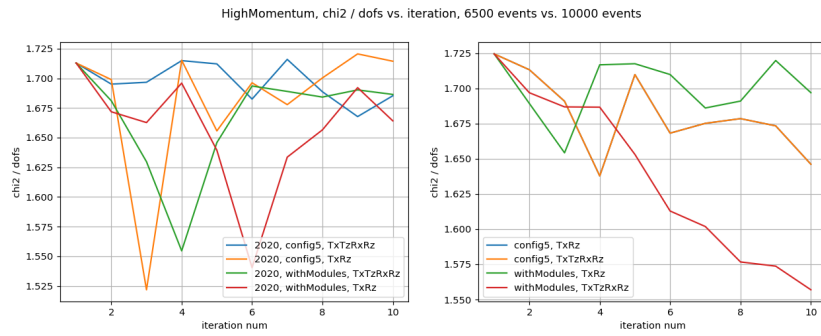


Abbildung 4.19: χ^2 versus iteration count normal(?).

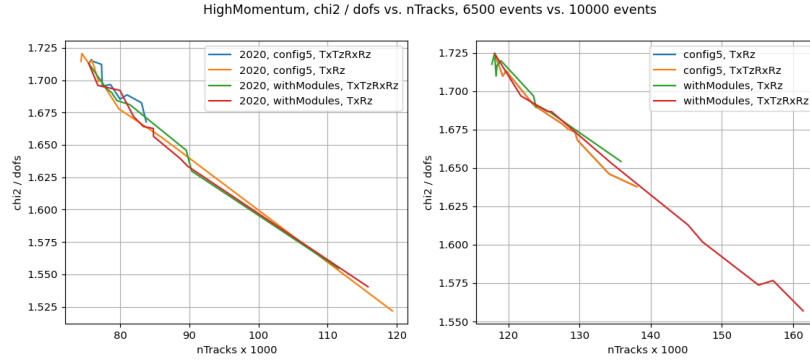


Abbildung 4.20: chi2 versus number of tracks normal.

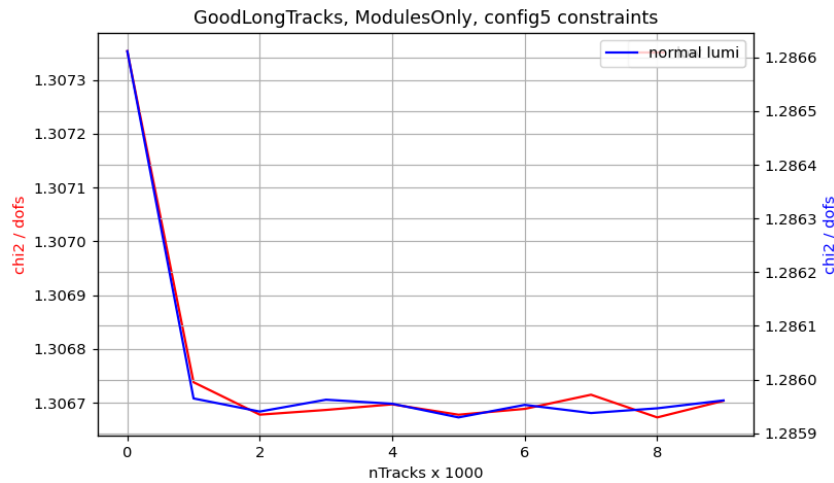


Abbildung 4.21: compare different luminosities and plot chi2 versus iteration number as a measurement for weakmodes and alignment.

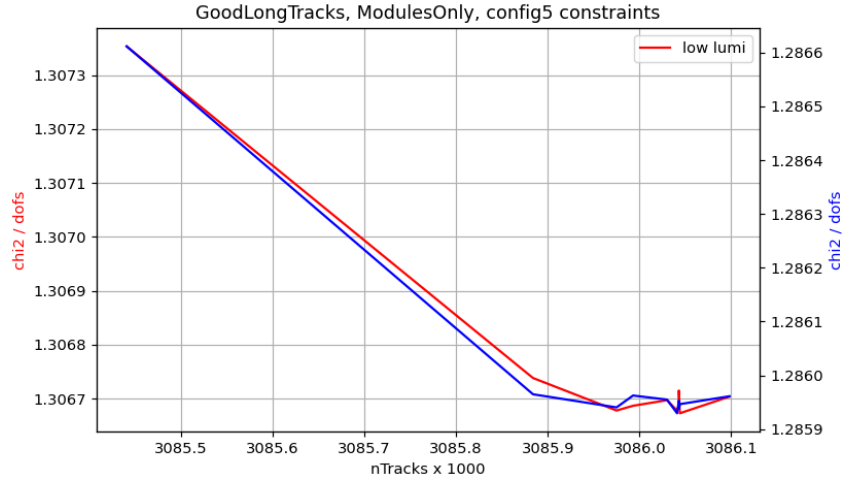


Abbildung 4.22: compare different luminosities and plot χ^2 versus number of tracks as a measurement for weakmodes and alignment.



Abbildung 4.23: compare different luminosities and plot number of tracks versus iteration number as a measurement for weakmodes and alignment.

4 Main part

january 24th: show that there is a visible difference between low and normal luminosity however the difference is not big enough to differentiate between the two phases during the ramp up and full run. therefore, for the upcoming analysis steps only the "normal/low" luminosity is taken into consideration.

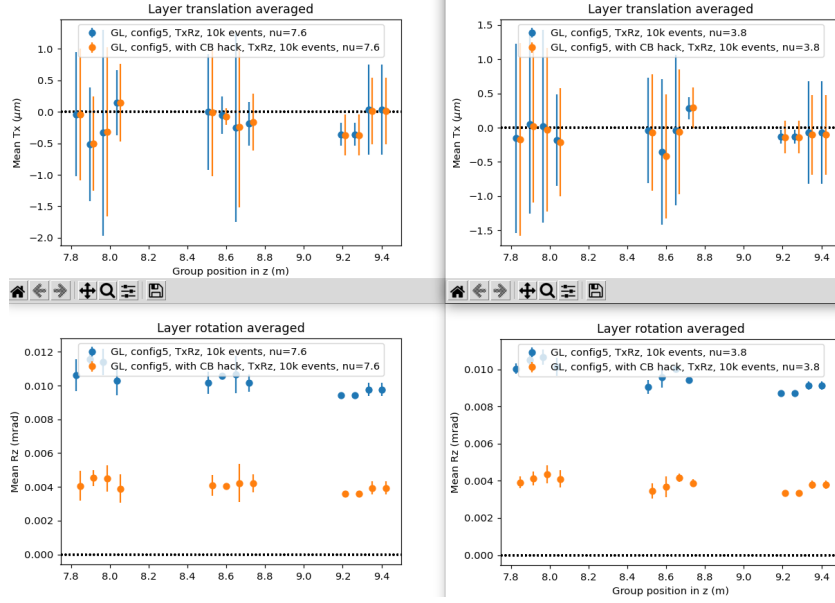


Abbildung 4.24: because of the clusterbias hack the difference between a measurement with the hack we implemented active and without is shown.

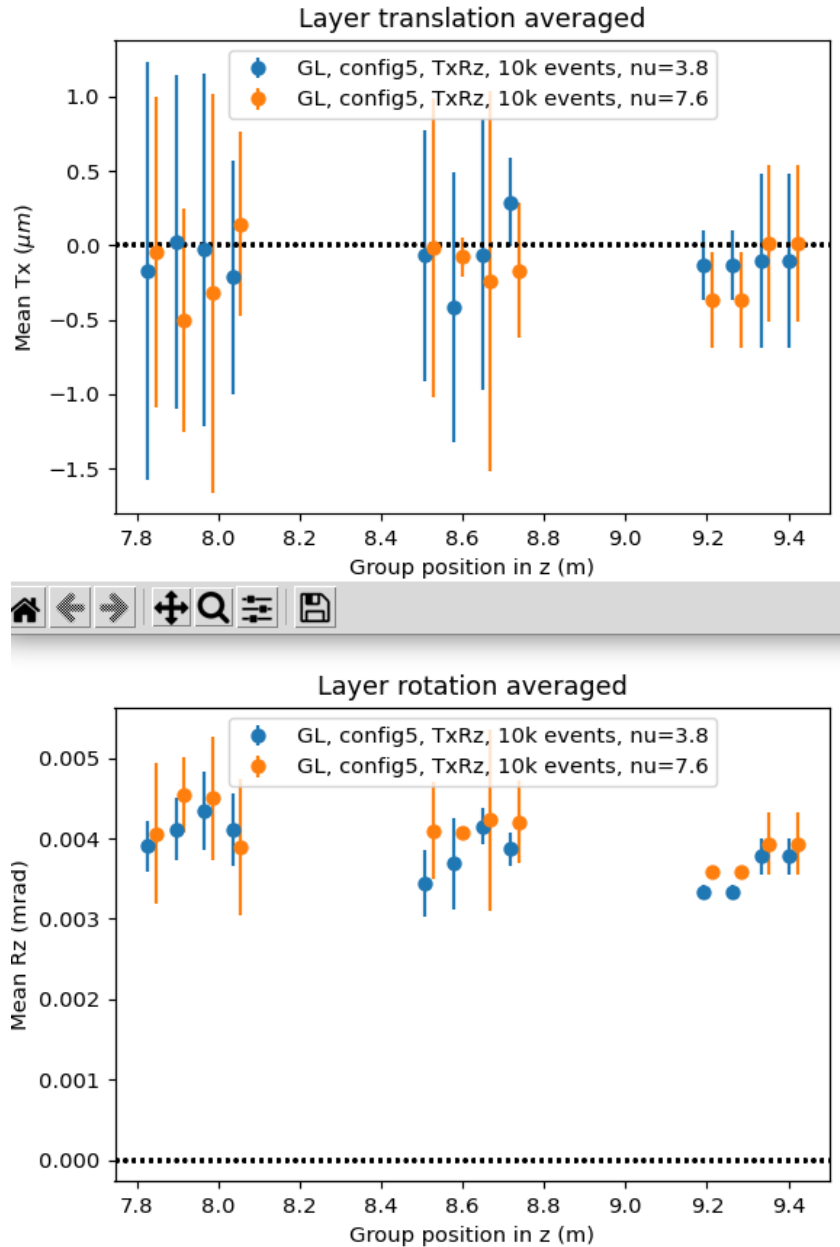


Abbildung 4.25: show difference between low and normal luminosity with clusterbias hack active.

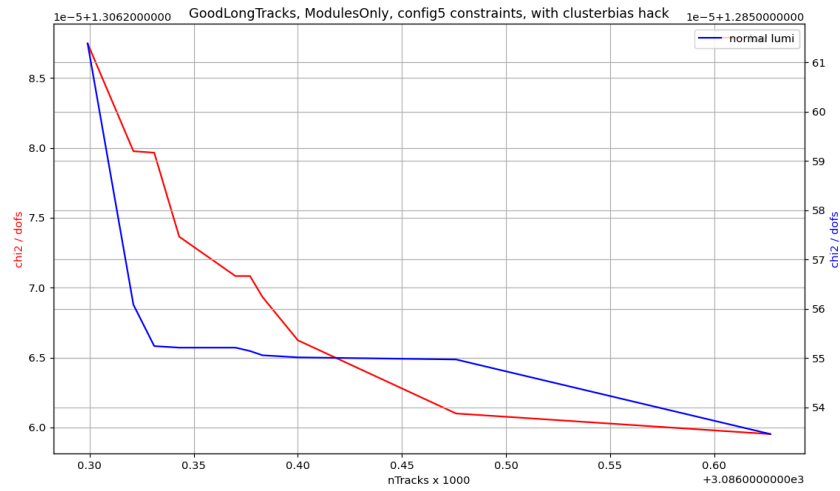


Abbildung 4.26: GoodLong tracks for module alignment and config 5 active. also the clusterbias hack is active comparing low and normal luminosity.

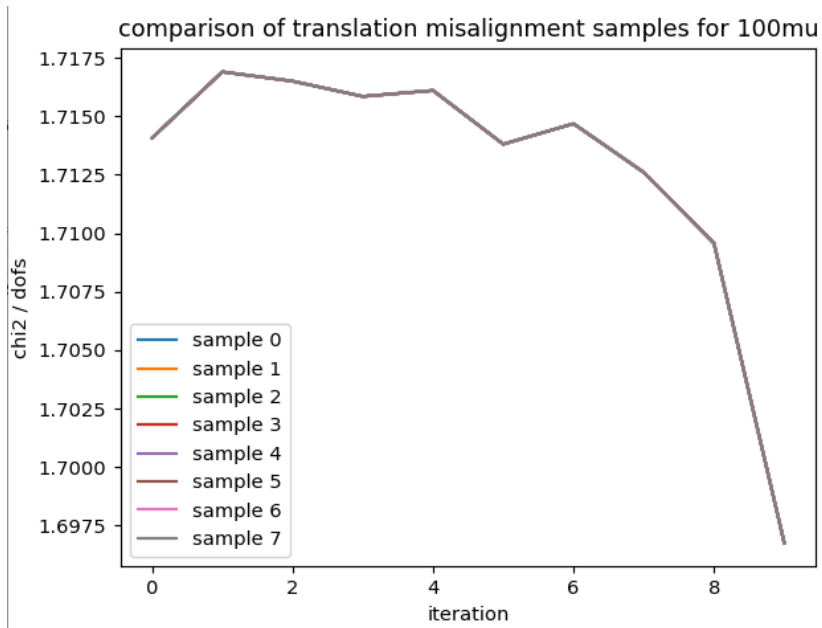


Abbildung 4.27: 100mu translation misalignment comparison for different misalignment samples.

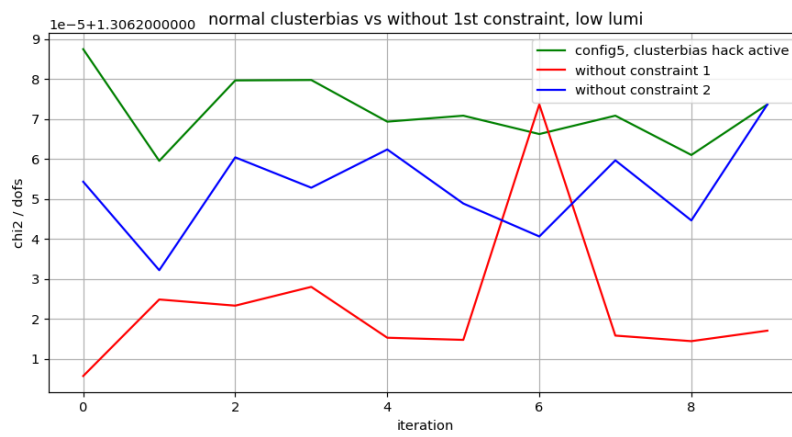


Abbildung 4.28: impact of removing constraints from existing studies regarding χ^2 .

5 Continuing Work

6 Future Work

instead of only doing normal(low) luminosity tests do it for the other luminosity as well (jan 24th)

7 Conclusion and Outlook

Literatur

- [1] *A diagram showing the complete structure of the LHC facility at CERN.* URL: https://www.researchgate.net/figure/A-diagram-showing-the-complete-structure-of-the-LHC-facility-at-CERN-There-are-the-4_fig8_348806406 (besucht am 09.03.2022).
- [2] *LHC Machine.* URL: https://cds.cern.ch/record/1129806/files/jinst8_08_s08001.pdf (besucht am 09.03.2022).
- [3] *LHCb Tracker Upgrade Technical Design Report.* URL: <https://cds.cern.ch/record/1647400/files/LHCB-TDR-015.pdf> (besucht am 09.03.2022).
- [4] *Physical Constants.* URL: <http://pdg.lbl.gov/2019/mobile/reviews/pdf/rpp2018-rev-phys-constants-m.pdf> (besucht am 11.08.2019).
- [5] *The invariant Rauch-Tung-Striebel Smoother.* URL: <http://ras.papercept.net/images/temp/IR0S/files/2526.pdf> (besucht am 24.03.2022).
- [6] *The LHCb Detector at the LHC.* URL: https://cds.cern.ch/record/1129809/files/jinst8_08_s08005.pdf (besucht am 09.03.2022).
- [7] J Van Tilburg. „Track simulation and reconstruction in LHCb“. Presented on 01 Sep 2005. 2005. URL: <https://cds.cern.ch/record/885750>.

Danksagung

An dieser Stelle möchte ich mich bei all denen bedanken, die mir während meiner Bachelorarbeit zur Seite standen und mich immer unterstützt haben.

Zuerst möchte ich mich bei Herrn Professor Dr. Kevin Kröninger bedanken, durch welchen ich an seinem Lehrstuhl meine Bachelorarbeit schreiben konnte. Außerdem möchte ich mich bei der Abteilung der ATLAS Datenanalyse für die konstruktiven Anregungen bedanken.

Einen großen Dank spreche ich vor allem meinem Betreuer Dr. Johannes Erdmann aus, der mich mit voller Unterstützung und wertvollen Ratschlägen und Hilfestellungen durch meine Bachelorarbeit begleitet hat. Durch ihn habe ich viel gelernt und bei Fragen konnte er mir stets weiterhelfen.

Ich möchte mich auch bei Herrn Professor Dr. Bernhard Spaan für die Zweitkorrektur meiner Arbeit bedanken.

Mein Dank gebührt außerdem Christopher Krause, Jan Lukas Späh, Michael Windau, Sebastian Lütge und Christian Beckmann für die fachliche Kompetenz bei Fragen aller Art.

Zuletzt möchte ich meiner Familie und Freunden dafür danken, dass sie mich während meines gesamten Studiums immer unterstützt und motiviert haben.

Eidesstattliche Versicherung

Ich versichere hiermit an Eides statt, dass ich die vorliegende Abschlussarbeit mit dem Titel „Alignment studies for the LHCb SciFi Detector“ selbstständig und ohne unzulässige fremde Hilfe erbracht habe. Ich habe keine anderen als die angegebenen Quellen und Hilfsmittel benutzt, sowie wörtliche und sinngemäße Zitate kenntlich gemacht. Die Arbeit hat in gleicher oder ähnlicher Form noch keiner Prüfungsbehörde vorgelegen.

Ort, Datum

Unterschrift

Belehrung

Wer vorsätzlich gegen eine die Täuschung über Prüfungsleistungen betreffende Regelung einer Hochschulprüfungsordnung verstößt, handelt ordnungswidrig. Die Ordnungswidrigkeit kann mit einer Geldbuße von bis zu 50 000,00 € geahndet werden. Zuständige Verwaltungsbehörde für die Verfolgung und Ahndung von Ordnungswidrigkeiten ist der Kanzler/die Kanzlerin der Technischen Universität Dortmund. Im Falle eines mehrfachen oder sonstigen schwerwiegenden Täuschungsversuches kann der Prüfling zudem exmatrikuliert werden (§ 63 Abs. 5 Hochschulgesetz –HG–).

Die Abgabe einer falschen Versicherung an Eides statt wird mit Freiheitsstrafe bis zu 3 Jahren oder mit Geldstrafe bestraft.

Die Technische Universität Dortmund wird ggf. elektronische Vergleichswerkzeuge (wie z. B. die Software „turnitin“) zur Überprüfung von Ordnungswidrigkeiten in Prüfungsverfahren nutzen.

Die oben stehende Belehrung habe ich zur Kenntnis genommen.

Ort, Datum

Unterschrift